Proceedings of the 9th U.S. National and 10th Canadian Conference on Earthquake Engineering
Compte Rendu de la 9ième Conférence Nationale Américaine et
10ième Conférence Canadienne de Génie Parasismique
July 25-29, 2010, Toronto, Ontario, Canada • Paper No 875

QUASI-STATIC AND PSEUDO-DYNAMIC TESTING OF ROCKING SPREAD FOOTINGS FOR BRIDGES

H. H. Hung [1], K. C. Chang[2], K. Y. Liu[1] and H.C. Wang[3]

ABSTRACT

From some of the actual engineering practices used in Taiwan, the size of spread footings was found to be exaggeratedly large due to the strict design provisions related to footing uplift. According to previous design code in Taiwan, the footing uplift involving separation of footing from subsoil is permitted only up to one-half of the foundation base area as the applied moment reaches the value of plastic moment capacity of the column. The reason for this provision is that rocking of spread footings is still not a favorable mechanism. However, resent researches have indicated that rocking itself may not be detrimental to seismic performance and in fact can act as a form of seismic isolation mechanism. In order to gain a better understanding of the problem of rocking, a series of rocking experiments were performed. Experimental data of six circular RC columns subjected to quasi-static and pseudo dynamic loadings were presented. During the tests, columns were rested on a rubber pad to allow rocking to take place. Experimental variables included dimension of footings, strength and ductility capacity of columns, and level of the earthquake intensity applied. Results of each cyclic loading test were also compared with the benchmark test with fixed base condition. By comparing the experimental responses of specimen with different design details, the beneficial effect of rocking in reducing ductility and strength demand of columns was verified. The energy dissipation from the inelastic rocking mechanism of the footing was also observed.

Introduction

Some of the retrofitting works for actual engineering practices in Taiwan resulted in uneconomically large spread footings. This is due to the restriction of footing uplift regulated in the bridge design code. The rocking mode of a spread footing induced by footing uplift is not favorable in the current design code. However, some researches have indicated that rocking itself can act as a form of isolation mechanism. The uplift of the footing can limit the earthquake forces that are transmitted to the column base, thereby possibly decreasing the plastic deformation that occurs in

[1] Associate Research Fellow, National Center for Research on Earthquake Engineering, Taipei, Taiwan
[2] Professor, Dept. of Civil Engineering, National Taiwan University, Taipei, Taiwan
[3] Graduate Student, Dept. of Civil Engineering, National Taiwan University, Taipei, Taiwan

the plastic zone. In addition, unless the footing is very massive, some uplift on the tension edge of the spread footing during a major earthquake cannot be avoided. The analysis of a design for seismic retrofitting that is based on the assumption that footing and soil is firmly bonded to each other will show unreasonable large internal forces in columns. To retrofit columns and their footings based on these unreasonable large internal forces will dramatically increase the cost of the retrofit. Besides, the widening and strengthening of the footing to restrain footing uplift will also force the columns to sustain most of the seismic energy and thereby intensify the damage level to those columns. For these reasons, and the fact that the retrofitting of a foundation can often be very expensive, it is reasonable to tolerate a certain amount of uplift of the footing in the retrofit design. In fact, foundation rocking has been conditionally accepted by some retrofitting guidelines.

On the other hand, in the current design philosophy for new bridges based on strength design approach, the rocking mechanism of the foundation is not allowed and is not taken into account in the analysis. This is because neglecting the effect of rocking will overestimate the seismic forces applied to the structures, and simply lean toward conservative side for the design. However, with the ever growing interest in performance-based design approaches in recent years, the seismic performance becomes the key parameter for design; thus, the importance of a precise prediction of the behavior of the structure subjected to seismic forces is increasingly being recognized. Not considering the effect of rocking sometimes underestimates the disadvantages that may be brought by rocking, such as large lateral displacements of the deck and permanent settlement in soils, and then leans toward unsafe design. Therefore, realistically taking the effect of rocking into consideration, including the interaction between foundation, column and soil, has gradually become an important issue in the seismic design for bridges.

The seismic isolation effect of the rocking mechanism has been identified in many previous researches since the pioneer work performed by Housner (1963), who noted that foundation uplift may explain the good performance of several elevated water tanks during the 1960 earthquake in Chile. Over the following few decades, several other articles were published on the study of rocking. Most of these earlier studies were performed by analytical approach, and few experimental studies were carried out. Recently, with the advances in experimental technique, rocking experiments became the focus of several studies, including series of tests performed on a large centrifuge by Gajan et al.(2008) and tests performed on a shaking table by Sakellaraki et al.(2005) and Espinoza and Mahin (2006). All of these previous studies recognized the beneficial effect of rocking. However, few of them considered the coupling effect of the material nonlinearity involved with column plastic hinging and the geometrical nonlinearity resulted from footing uplift. Also, the relevant researches are not sufficiently comprehensive to provide confidence to revise the design code extensively. In order to have a better understanding about the rocking mode and its role on the overall behavior of a bridge, more experimental data are still required. Therefore, in this study, six circular reinforced concrete columns with spread footings and different design details were constructed and subjected to a series of rocking experiments. These experiments include pseudo-dynamic test and cyclic loading test.

Theoretical Calculation for Rocking Mechanism

In order to make sure that the experiment can achieve the goal to investigate the coupling effect of the material nonlinearity from column hinging and the geometrical nonlinearity from footing uplift, before the experimental specimens were designed and constructed, the basic

theory for rocking mechanism was studied and a simple calculation was performed. For a column with a spread footing standing on soils, the footing will lift off the ground once its moment of resistance provided by gravity is overcome. Thus, the base moment of the foundation can be limited to the value required to induce uplift against the restraining forces due to gravity. By assuming that the underlying soil is a perfect plastic material with an ultimate stress of q_y, according to the force equilibrium, the limit value of the moment of a rigid foundation can be written as

$$M_2 = \frac{BW_T}{2}\left(1 - \frac{q}{q_y}\right) \tag{1}$$

where B is the width of the footing in the direction of the bending; W_T is the total axial load applied to the foundation base; q is the contact stress under the foundation and equal to W_T/BL, in which L denotes the length of the foundation. This limitation of moment also imply that if the footing of a column is allowed to rock with the uplift, the shear force and bending moment that the column has to sustain will also have an upper limit value. The upper limit value for the shear force and bending moment at the column base can be derived from value M_2,

$$V = \frac{M_2}{H} = \frac{BW_T}{2H}\left(1 - \frac{q}{q_y}\right) \tag{2}$$

$$M = V(H - h) = \frac{BW_T}{2H}(H - h)\left(1 - \frac{q}{q_y}\right) \tag{3}$$

Where H is the distance between the location where the lateral force applies and the foundation base, and h is the height of the foundation. If we further assume that the ultimate stress of q_y is far larger than q, then the value of q/q_y in Eqs. (2) and (3) can be omitted and the limit values of the shear force and the bending moment that the column will sustain depend only on the footing size and the total vertical force of gravity. Obviously, the ratio of the strength capacity of the column to the upper limit moment calculated in Eq. (3) is the key parameter for the seismic performance of the column with a spread footing. It is expected that once the bending moment capacity of the column is larger than the limit value M calculated by Eq. (3), the response behavior of the column-footing system will be govern by rocking of the footing, and the plastic deformation will not be formed at the column base. On the other hand, if the bending moment capacity of the column is much lower than the base moment that is required to induce uplift, the rocking mechanism will not be triggered, and the column with spread footing would response like the same column with fixed base. However, if the bending moment capacity of a column is only a little bit lower than the upper limit value M, it is highly likely that both the material nonlinearity involved with column plastic hinging and the geometrical nonlinearity due to footing uplift will help to dissipate some energy.

Experimental Program

Test Specimens

Based on the simple calculation in the previous section, six reinforced concrete columns with two types of foundation size and three types of design details in column base were designed and constructed. As shown in Fig. 1, these circular RC columns are all 50 cm in diameter with a

clear height of 2.5 m and a height of footing 0.5 m. Their footing sizes are either B = 140 cm or B = 170 cm. Thus, according to Eq. (3), the corresponding upper limit value of bending moment for specimens with a smaller footing (B = 140 cm, W_T = 574 kN) is M = 334.8 kN-m. As for the specimens with a larger footing (B = 170 cm, W_T = 585 kN), the corresponding upper limit value is M = 414.4 kN-m. In order to compare the rocking performance of specimens with different ratios of the moment capacity of the column to the upper limit moment M, these test columns were reinforced with three types of design details. One with 12-D19 (steel ratio = 1.75%) main reinforcements was transversely reinforced with D13 perimeter hoops spaced 9 cm (volumetric confinement ratio ρ_S = 0.012), corresponding to a case with sufficient transverse reinforcements. The other two with 18-D19 (steel ratio = 2.63%) main reinforcements were transversely reinforced with D13 perimeter hoops spaced 9 cm and 18 cm, respectively. The one with the transverse reinforcements spaced 18 cm represents a column with an insufficient volumetric confinement ratio (ρ_S = 0.006). The nominated material properties for these specimens are as follows: concrete compressive strength f_c'=280 kg/cm^2; yield strength of main reinforcements F_y=4200 kg/cm^2; yield strength of transverse reinforcements F_{yh}=2800 kg/cm^2. Based on the nominated material properties, the moment capacity of these specimens was also calculated from moment curvature analysis. The effective yield moments for specimens with 18-D19 and 12-D19 main reinforcements are 428.3 kN-m and 329.0 kN-m, respectively.

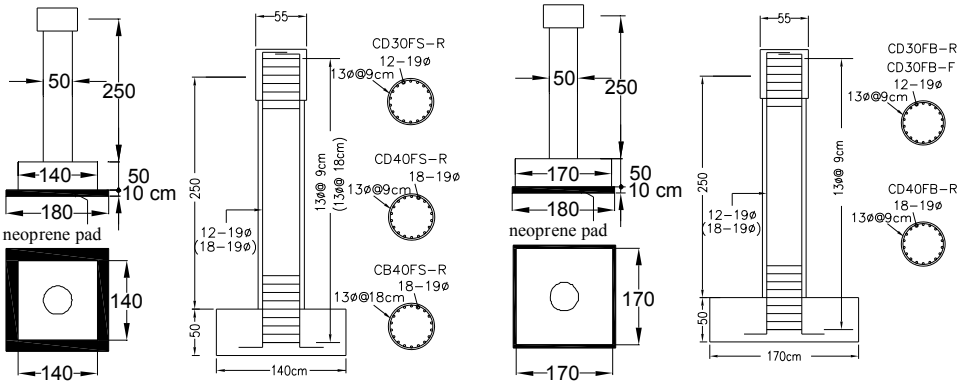

(a) (b)

Figure 1 As-built details of model columns (a) B=140cm, (b) B=170cm

With the combination of different footing size and design details, a total of six test columns were designed and named as CD40FS-R, CB40FS-R, CD30FS-R, CD40FB-R, CD30FB-R and CD30FB-F, respectively, as plotted in Fig. 1 and listed in Table 1. In which, characters “FS” and “FB” are denoted as cases with a footing of smaller size (B=140 cm) and of larger size (B=170 cm), respectively. Number “40” and ”30” are denoted as cases with 18-D19 and 12-D19 main reinforcements, respectively; characters “CD” and “CB” are denoted as columns transversely reinforced with perimeter hoops spaced 9 cm and 18 cm, respectively; while “R” and “F” represent rocking base condition and fixed base condition, respectively. By so setting, the ratios of the moment capacity of the column to the upper limit moment M for CD40FS-R, CD40FB-R, CD30FS-R and CD30FB-R are 1.28, 1.03, 0.98 and 0.79, respectively. Specimen CB40FS-R has the same ratio of CD40FS-R. Thus, the ratios for these specimens cover values higher than 1, and less than 1.

Test Setup

To clarify the difference in response behavior between columns with a rocking-base condition and those with a fixed-base condition, both tests with and without the footing uplift restraint were conducted. Fig. 2 illustrates the test setup. In the case where footing uplift was restrained, four tie-down rods were placed through the footing and anchored into the strong floor of the laboratory to restrain the rocking mode of the foundation (Fig. 2b). In the case where the rocking mechanism was considered (Fig. 2a), the square footings were rested on a 10 cm thick neoprene pad (Duro-60), simulating a spread footing foundation in a stiff soil. The size of the neoprene pad was 180cm×180cm. During the test, the lateral deformation of the neoprene pad was restrained. In addition, a special apparatus with rolling balls were installed on each side of the foundation to prevent torsion of the test column but allowed uplift of the footing.

Table 1. Design details and experimental test schedule

Test Specimens	Design details	Base condition	Tests
CD40FS-R	Footing: 140cm×140cm 18-D19 with stirrup: D13@ 9cm	Rocking base	pseudo-dynamic test (TH1,TH2)
			cyclic loading test
		Fixed base	cyclic loading test
CD30FS-R	Footing: 140cm×140cm 12-D19 with stirrup: D13@ 9cm	Rocking base	pseudo-dynamic test (TH1,TH2)
			cyclic loading test
CD40FB-R	Footing: 170cm×170cm 18-D19 with stirrup: D13@ 9cm	Rocking base	pseudo-dynamic test (TH1,TH2)
			cyclic loading test
CD30FB-R	Footing: 170cm×170cm 12-D19 with stirrup: D13@ 9cm	Rocking base	pseudo-dynamic test (TH1,TH2)
			cyclic loading test
CB40FS-R	Footing: 140cm×140cm 18-D19 with stirrup: D13@ 18cm	Rocking base	cyclic loading test
		Fixed base	cyclic loading test
CD30FB-F	Footing: 170cm×170cm 12-D19 with stirrup: D13@ 9cm	Fixed base	cyclic loading test

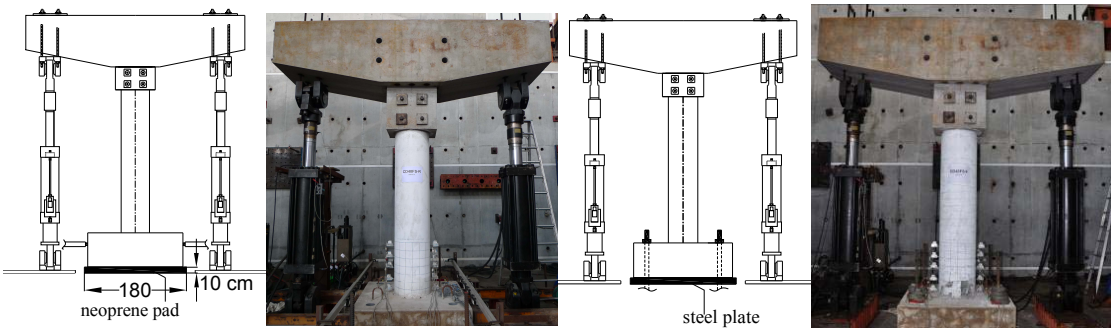

(a) (b)

Figure 2 test setup (a) rocking bas; (b) fixed base.

During the test, an axial load of 539 kN was applied to the test column through a tap beam using two vertical actuators. The vertical loading was kept constant throughout the test to simulate the tributary dead load of the deck, which is around $0.10A_g f_c'$, where A_g is the gross cross-sectional area of the column. One horizontal actuator was used to apply the lateral force to the column's top to simulate the seismic loading. The location of the application force was 2.5 m from the top of the footing, and 3 m from the footing base.

Test Schedule

The test schedule is also listed in Table 1, which includes pseudo-dynamic loading test and quasi-static cyclic loading test. The input ground motions for pseudo-dynamic test and lateral loading sequence for cyclic loading test are all shown in Fig. 3. The input ground motions are two artificial earthquake accelerations. One is a code-compatible medium earthquake acceleration (TH1) and the other is a code-compatible design earthquake acceleration (TH2) for Nantou Pouli, a region of high seismicity in Taiwan. As shown in Fig. 3, the peak ground motion for TH1 and TH2 are PGA=100 gal and 326gal, respectively, and the cyclic tests were performed under displacement control to a drift ratio of 7% (17.5cm). For specimens CD40FS-R, CD30FS-R, CD40FB-R and CD30FB-R, the columns were firstly tested sequentially by two pseudo-dynamic loadings, i.e., TH1 and TH2, under the rocking base condition. Then, the same specimens and another specimen CB40FS-R were subjected to a cyclic loading test. After these tests performed in rocking base condition were competed, since no physical damage can be observed in specimens CD40FS-R and CB40FS-R, the same specimens were later constrained to the strong floor and tested by another cyclic loading test, acting as benchmark tests with fixed base condition. Another specimen CD30FB-F that has the same design details as specimen CD30FB-R was also tested by a cyclic loading test under fixed base condition to represent a benchmark test of columns with 12-D19 main reinforcements.

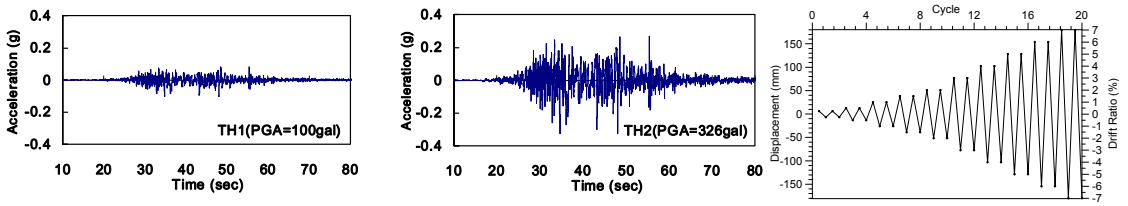

Figure 3 Input ground motions for pseudo-dynamic tests and loading sequence for cyclic loading test

Test Results and Discussions

Pseudo-dynamic tests of TH1 and TH2

As mentioned previously, specimens CD40FS-R, CD30FS-R, CD40FB-R and CD30FB-R were firstly supported on a neoprene pad without uplift restraint and subjected to the pseudo-dynamic test of TH1. The hysteretic responses of these tests are plotted in Fig. 4. In which, figure (a) shows the lateral load versus the lateral displacement curves for the system, and (b) shows the moment versus rotation curves at the column base. In these moment-rotation curves, the rotations were obtained by taking the reading of the highest tiltmeter located at a height of 65 cm minus the reading of another tiltmeter mounted on the footing. Thus, the rotations in Fig. 4(b) come from the elastic and plastic flexure of the column only; whereas the lateral displacements given in Fig. 4(a) come from the elastic and plastic flexure of the column plus the rocking of the footing. From these figures, it is evident that under the subjection of TH1 acceleration, both the force-displacement curves and the moment-rotation curves almost remain linear. This result indicates that the uplift of footing was not significant and the plastic hinge was not formed while the columns experienced this minor earthquake. Other phenomenon can be observed in Fig. 4 is that the response behaviors of the specimens with the same size of footing were similar. That is to say, specimens CD40FS-R and CD30FS-R had similar response behavior, and specimens CD40FB-R and CD30FB-R also behaved similarly, even though their design details of main reinforcements were different. This observation implies that the control parameter for the

performance of these test columns subjected to such a minor earthquake is the dimension of the foundation, but not the strength capacity of the column.

After the pseudo-dynamic test of TH1, these four specimens were subjected to another pseudo-dynamic test of TH2. The experimental results of the lateral force versus the lateral displacement curves and the moment versus the rotation curves are plotted in Figs. 5(a) and 5(b), respectively. By observing Figs. 5(a) and (b), it is evident that under the subjection of a design earthquake, the plastic deformation of the columns were still not noticeable. However, at the same time, some uplift already occurred since the lateral force-displacement curves are not linear anymore, but shows a softer stiffness as the lateral displacement increases. This observation implies that some uplift occurred during the subjection of this design earthquake, and provided some isolation effect. Again, the response behaviors of specimens CD40FS-R and CD30FS-R are almost the same, even though the numbers of their main reinforcements are different. As for the specimens with B = 170 cm, the maximum values of lateral force and moment of specimen CD30FB-R are a little bit lower than that of specimen CD40FB-R. Also, the area enclosed by the hysteresis loop of the moment-rotation curve for specimen CD30FB-R is a little bit larger than that of CD40FB-R. This is because CD30FB-R has a moment strength less than that of CD40DB-R, and it already yielded a little bit before the base moment due to rocking could reach its upper limit value.

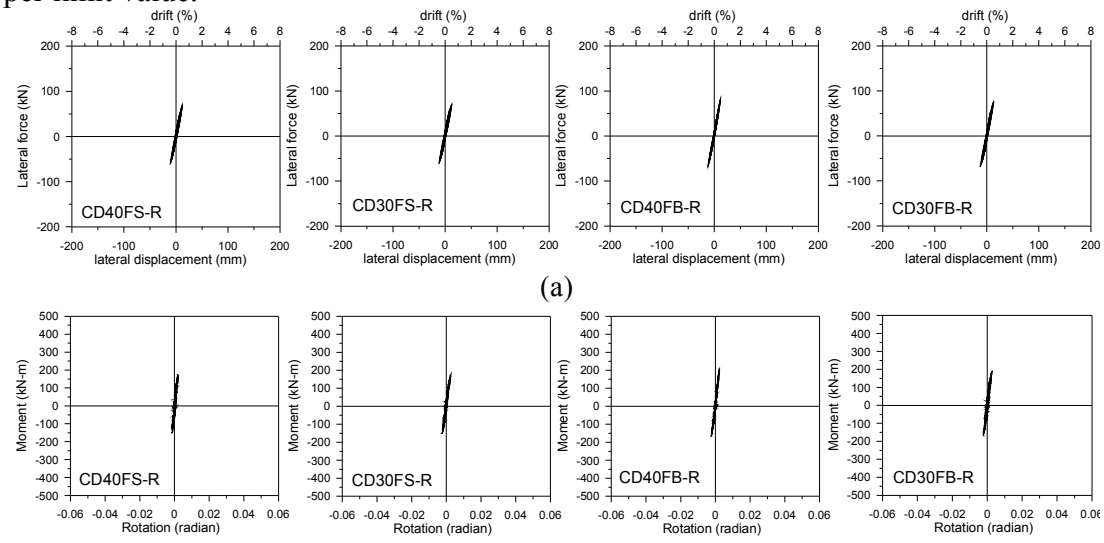

Figure 4 Experimental results for pseudo-dynamic test of TH1: (a) lateral load vs. displacement; (b) moment vs. rotation at column base

Cyclic loading tests

According to the experimental test schedule, a total of eight cyclic loading tests were performed. Fig. 6 and Fig. 7 show the experimental results for specimens with 18-D19 and 12-D19 main reinforcements, respectively. Again, Figs. (a) and (b) are lateral force vs. lateral displacement curves and moment vs. the rotation curves, respectively. In these figures, the results for fixed base cases of CD40FS-F, CB40FS-F and CD30FB-F can signify the capacity of columns, as well as represent cases with a footing of very large size. For instance, CD40FS-F in Fig. 6 can represent a case with the same design details as CD40FB-R and CD40FS-R, but with a massive footing. In addition, CD40FS-F can signify the capacity of specimens with 18-D19 main

reinforcements. It should be noted that because the actual material properties for the specimen is higher than the designed one, the capacity of specimen CD40FS-F shown in Fig. 6 is higher than what was calculated based on the design nominated properties. By comparing the results of CD40FS-F, CD40FB-R and CD40FS-R, it is noted that the rocking behavior becomes more pronounced as the dimension of footing decreases. Also, the maximum value of lateral forces that the column sustained decreases with the decrease in footing size. These corresponding maximum values for CD40FB-R and CD40FS-R shown in Fig. 6(a) are respectively around V = 160 kN and V = 130 kN, close to the upper limit values calculated by Eq. (2). Besides, the maximum value of the bending moment that the column sustained decreases too, as shown in Fig. 6(b). Because the maximum values of moment sustained by CD40FB-R and CD40FS-R are less than the moment capacity of columns indicated by CD40FS-F, the moment-rotation curves for both CD40FB-R and CD40FS-R are almost linear, implying that not much plastic deformation occurred in columns. As for the cases with insufficient transverse reinforcements, CB40FS-F is the benchmark test for CB40FB-R. Similarly, the results show that with the decrease in footing size, the rocking behavior becomes more obvious. The seismic force that the column sustained was limited to an almost constant value around V = 130 kN and M = 320 kN-m for the rocking cases of CB40FS-R. Because the maximum value of bending moment sustained by the column was lower than its moment capacity in column base indicated by CB40FS-F, the corresponding moment-rotation curve shown in Fig.(b) for CB40FS-R are almost linear. Another trend can be observed in Fig. 6 is that the response behaviors of CD40FS-R and CB40FS-R are similar, even though the responses of CD40FS-F and CB40FS-F are different. This result confirms that the ductility demand of a column can be reduced if its upper limit value of moment due to rocking is lower than the moment capacity of the column base.

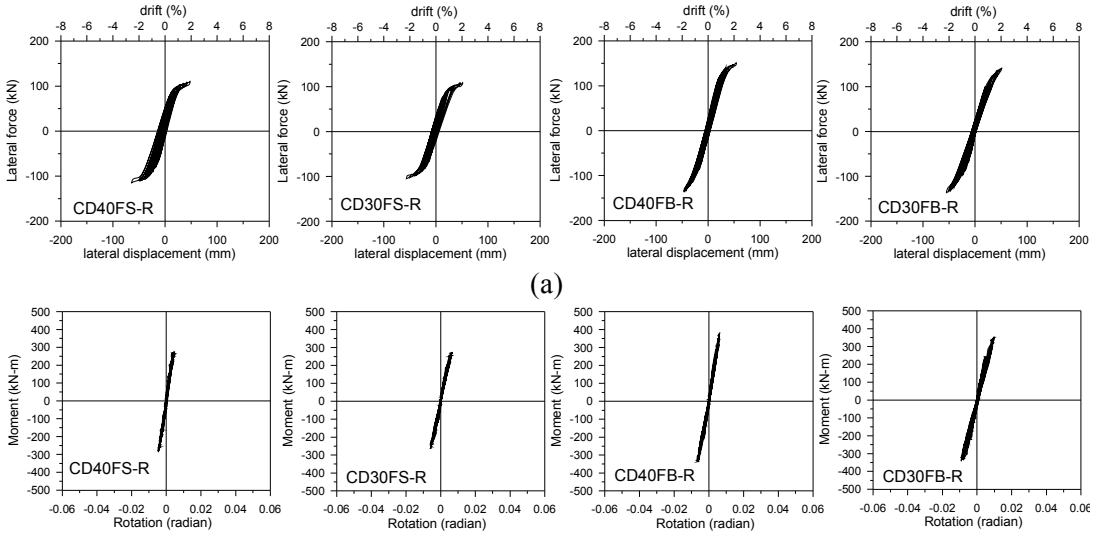

Figure 5 Experimental results for pseudo-dynamic test of TH2: (a) lateral load vs. displacement; (b) moment vs. rotation at column base

Fig. 7 plots the experimental results for specimens with 12-D19 main reinforcements. CD30FB-F is the benchmark test, representing the case with a footing of very large size and signifying the capacity of specimens with 12-D19 main reinforcements. The results demonstrate that with the decrease in footing size, the nonlinear rocking behavior becomes more significant. Consequently, the plastic deformation occurred in column base becomes minor. For instance, the

moment-rotation curve for CD30FS-R is almost linear, while some plastic deformation was formed in CD30FB-R. For CD30FB-R, the calculated upper limit value of moment based on Eq. (2) is 414.4 kN-m, a value higher than the moment capacity of column indicated by CD30FB-F. Therefore, before the base moment of the footing could reach its limit value, the column already yielded, and the moment strength of the column governed the response behavior. On the other hand, for specimen CD30FS-R, the maximum value of bending moment sustained by column was around 320 kN-m, a value lower than the effective yield moment of CD30FB-F. Thus, the column can still remain in elastic state.

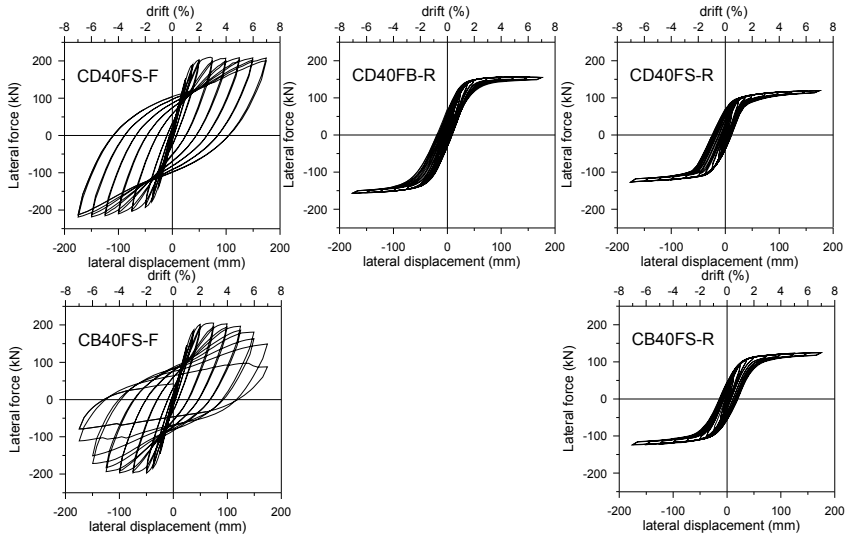

(a)

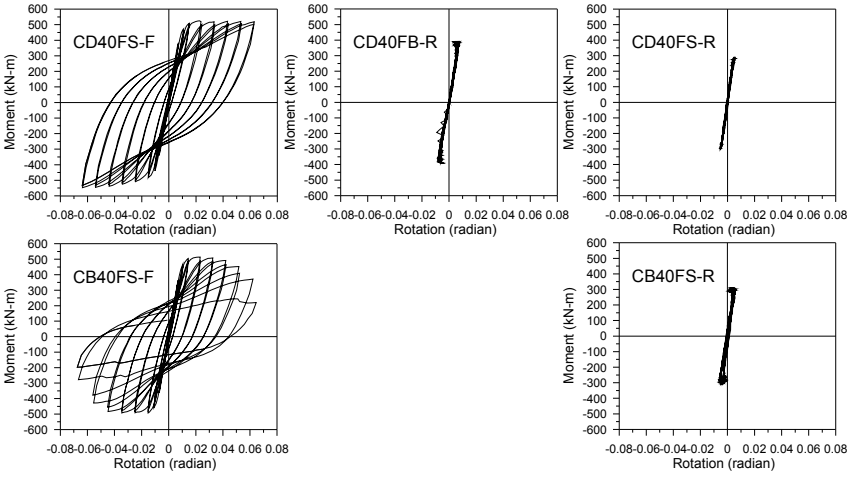

(b)

Figure 6 Experimental results for cyclic loading test of specimens with 18-D19 main reinforcements: (a) lateral load vs. lateral displacement;(b) moment vs. rotation at column base

Conclusions

In this study, a series of pseudo-dynamic and cyclic loading tests of six reinforced concrete columns with different size of footing, different strength and ductility capacity were conducted. These experiments showed that if the footing of the column is allowed to rock, the moment that the column has to sustain can be limited to a certain value. This upper limit value

can be calculated based on a simple equation only related to the footing size and the total vertical force of gravity. If this limit value for moment is lower than bending moment strength of the column, the plastic deformation will not be formed at the column base and the ductility demand of the column can be reduced. In addition, results also shows that if the footing uplift took place, there was a decrease in plastic deformation at the plastic hinge of a column as a result of the energy dissipation of the inelastic rocking mechanism. The extent of decrease in plastic deformation depends on the ratio of the moment capacity of column to the limit value of moment that the column sustained.

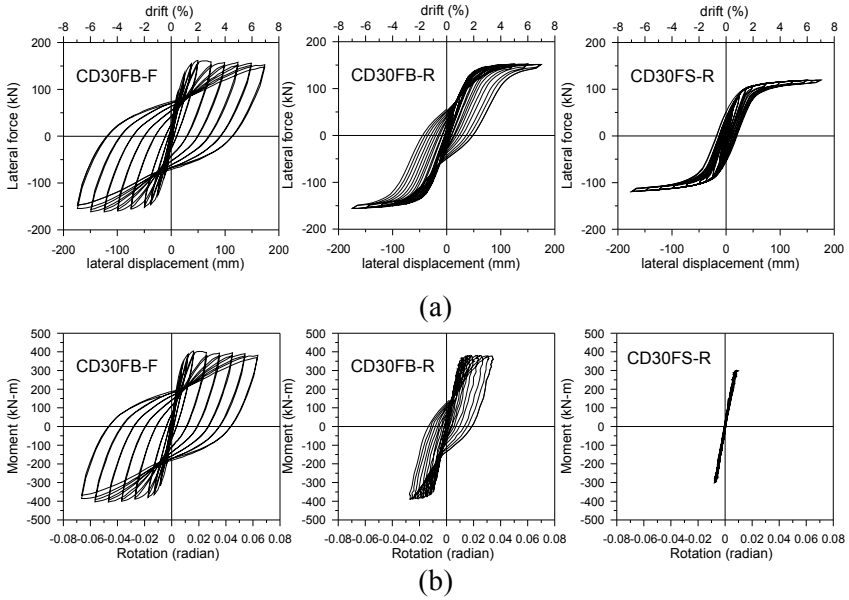

Figure 7 Experimental results for cyclic loading test of specimens with 12-D19 main reinforcements: (a) lateral load vs. displacement ; (b) moment vs. rotation at column base

Acknowledgments

The study reported here was funded in part by the National Science Council of Taiwan under grant number NSC 97-2625-M-492-004. The test specimens, facilities and technical support from the National Center for Research on Earthquake Engineering are also gratefully acknowledged.

References

Housner, G. W., 1963. The behavior of inverted pendulum structures during earthquakes. *Bulletin of the Seismological Society of America*, 53(2), 403-417.

Gajan, S., and B. L. Kutter, 2008. Capacity, settlement, and energy dissipation of shallow footings subjected to rocking. *Journal of Geotechnical and geoenvironmental engineering* (ASCE); 134(8),1129-1141.

Sakellaraki, D., G. Watanabe, and K. Kawashima, 2005. Experimental rocking response of direct foundations of bridges. S*econd International Conference on Urban Earthquake Engineering*, Tokyo Institute of Technology, Tokyo, Japan, March 7-8, 497-504,

Espinoza, A. and S. Mahin, 2006. Rocking of bridge piers subjected to multi-directional earthquake excitation. *Fifth National Seismic Conference on Bridge & Highways*, San Francisco, CA, September 18-20.